

# MODELING AND SIMULATION OF AN INDUCTION MACHINE WITH A NOVEL CONCEPT OF A CONVERTER-FED ROTOR

P.Mahesh Kumar<sup>1</sup> | M.L.Dwarakanand<sup>2</sup>

<sup>1</sup>(M.Tech Scholar, Dept of EEE, Global College of Engineering & Technology, Kadapa, A.P, India)

<sup>2</sup>(Asso. Professor & HOD, Dept of EEE, Global College of Engineering & Technology, Kadapa, A.P, India)

**Abstract**—This paper investigates an induction machine with a novel concept of the rotor fed by a converter. The stator is Y connected and directly connected to the grid, while the rotor windings are open-ended and fed by a back-to-back converter with a floating capacitor. Power factor and efficiency improvements of the induction motor are studied with different settings of phase-shift angle between the two converters. Moreover, the dynamic performance of the induction machine is explored in MATLAB/Simulink and verified experimentally on a 1.8-kW induction machine in the laboratory. The result shows good agreement between simulation and experiment. At a constant speed, variable load operation of the induction machine is obtained by setting the frequency of the rotor voltage.

**Keywords**— Back-to-Back Converter; Dynamic Performance; Induction Machine Drives; Open-End Winding and Unity Power Factor

## 1. INTRODUCTION

The Induction machine is generally used in industry since of its reliability, robustness and cost effectiveness. One inherent drawback of induction machines is that they describe reactive power from the grid and the power factor can be poor. Especially when the machine start or operates with light loads, power factor and efficiency are drastically reduced. Power factor improvement of induction machine is thus attractive and has been pursued for decades. The simplest way to compensate the reactive power is to connect capacitor banks at the machine terminals. However, an unsuitable selection of capacitance may result in overvoltage due to self-excitation when the machine is disconnected from the supply, which could damage the machine. This approach is not flexible since different capacitances are needed when the loading condition changes. A scheme of supplying variable capacitance is proposed, where the induction machine is straightforwardly associated with the network while a three stage pulse width modulation (PWM) converter with a gliding capacitor is associated at the acceptance machine terminals. Be that as it may, the enhanced power factor is acknowledged just for the network yet not for the induction machine itself. The losses in the machine are not reduced thus the machine still suffers from poor power factor and hence poor efficiency. In the 1980s, as an alternative to improve the mains power factor, the stator windings of a cage-rotor induction machine were rewound to achieve unity power factor. The stator windings were divided into two groups with different number of turns. The two sets of windings were electrically connected. This attracted a lot of interest at that time. Different connections of two sets of identical stator windings are investigated. The results from both show that the mechanical output capability of the rewound induction machine is reduced compared with the original machine. With the development of power electronics, topologies using rectifiers and inverters become interesting. In one of these topologies, a rectifier is associated with the matrix

and supplies a dc voltage to the PWM inverter associated with the stator of enlistment machine. The power factor of the acceptance machine can be enhanced by managing the PWM inverter yield voltage to the stator windings. Besides, the rectifier can be supplanted by a converter which empowers the bidirectional power stream between the matrix and induction machine thereby increasing the power factor. However, harmonics are introduced to the power network because of the switching power devices. A topology with a high frequency ac link between grid and machine side converters and other filters are investigated to reduce the current harmonics. Instead of directly connecting the capacitors to the machine or the power network to increase power factor and reduce harmonics, an extra set of stator winding is introduced to supply the required equivalent capacitance to the stator circuit. This is referred to as the dual stator winding induction machine. Two electrically secluded but magnetically coupled three-phase windings are installed in the stator in the mentioned induction machine. The two sets of windings can be designed to have the equal or dissimilar pole and phase numbers. The main winding is coupled to the grid while the auxiliary winding is associated to a three-phase PWM converter with a floating capacitor. Power factor improvement can be obtained by introducing a proper capacitance to the induction machine through the converter using a suitable modulation method. Alternatively, the auxiliary stator winding can be avoided and the three-phase converter is connected to the stator by accessing the Y-point of the stator windings. The converters in the above mentioned topologies need to be dimensioned for rated voltage to enable the machine to operate over the complete load range. Furthermore, the induction machine can be energized from the rotor side on account of an injury rotor acceptance machine, for example, the doubly-fed induction machines (DFIM). Particularly, solidarity control factor can be acquired inside 25% to 100% of the appraised mechanical power with the assistance of an outside exciter offering the consecutive converter to the rotor of the

enlistment machine. This topology is fit for controlling both dynamic and responsive power, and consequently also the power factor. However, power factor improvement in DFIM requires closed loop control where the exact location of the flux vector is needed. Another recent novel topology for power factor improvement is proposed, in which a back-to-back converter with a floating capacitor is related to the rotor windings. Power factor enhancement can be achieved by magnetizing the machine from the rotor side with the reactive power supplied by the rotor-connected converter. It should be noted that, unlike the DFIM, the topology can only deal with the reactive power since the dc-link only contains a floating capacitor. However, the power factor will be improved automatically in this topology with open loop control. Specifically, the power factor of the induction machine at certain speed and load can be calculated with known machine parameters. Studies on the topology proposed explain that the stator power factor can be enhanced over a wide variety of load torque. In this paper, the impact of changing the phase-shift angle among the two back-to-back connected converters on power factor improvement is further studied. Efficiency improvement for the induction machine as well as the whole system is also studied. Moreover, dynamic performance of the induction machine including starting, loading and load changing is investigated through simulation.

## 2. CONTROL OF DFIG

Control of the DFIG is more confused than the control of a standard enlistment machine. With a specific end goal to control the DFIG the rotor current is controlled by a power electronic converter. One regular method for controlling the rotor current is by methods for field-oriented (vector) control. A few vector control plans for the DFIG have been proposed. Vector control strategies, utilizing Park changes permit decoupling control of dynamic and receptive power. Notwithstanding accomplishing decoupled control of dynamic and responsive power through vector control technique, various other control aims can be realized. These control aims may include but not limited to decoupled control of torque and power factor, slip power recovery control, control of rotor current.

### 2.1 Controller principles

In order to apply vector control for effective control of DFIG, the rotor current is decayed into dq-tomahawks segments for free control of torque, dynamic power and receptive power. The present control must be sufficiently quick, with the goal that the static inverter carries on like a present hotspot for the external control circles. Two noteworthy control plans accessible for compelling direction of the current-managed enlistment machines are hysteresis controller and synchronous PI controller. Two other controller methods similarly being used incorporate least time control and model-reference versatile control. Synchronous PI controllers and least time control both work with arrived at the midpoint of voltages and streams.

### A. Hysteresis control

Hysteresis control also called tolerance-band or dead-band control is a feedback controller that switches abruptly between two states. The hysteresis controller can be made with either a current- or a voltage loop. In a current-loop hysteresis control, the actual current is compared with a given current signal and if the actual current signal exceeds the given current signal, the switching state of the system is changed to control the change in actual current signal in order to track the given current signal.

### B. Synchronous PI controllers

This is one of the most popular control methods. The idea is to transform currents and voltages into a rotating reference frame, where the controlled currents are constant in steady-state, use the PI controllers on the transformed values, and transform the controller outputs back to the stationary reference frame. When the reference signal is constant, zero steady-state error is achieved by the integral term of the controller. When the reference current is a sinusoidal signal however, straightforward use of the PI controller would lead to steady-state error due to the finite gain at the operating frequency. For these situations PR-controllers are proposed, which have infinite gain at a specified frequency. The drawbacks are the nonlinearities introduced in the transform and less than optimal control performance. The advantage is that it is simple to understand and simple to implement.

### C. Minimum time control

This controller uses reactive power impulses to improve the transient response. It has been proved to be slightly better than synchronous PI control.

### D. MRAS

Model-reference adaptive control has the advantage of not having to know the process parameters exactly, while still achieving good performance.

## 3. PROPOSED SYSTEM

In the presented topology, shown in Fig. 3.1, the stator windings are Y-connected with the three phases directly connected to the grid. Each of the three rotor phase windings are short-circuited via a back-to-back converter, as shown in Fig. 3.2. Hence, it is possible to magnetize the induction machine from the rotor side. The converter is connected to the rotor windings through slip rings and controlled by a dSpace controller box. The switching signals are divided into two groups, one for each converter. Sinusoidal SPWM strategy is applied to the two voltage source converters with the same switching frequency and modulation index.

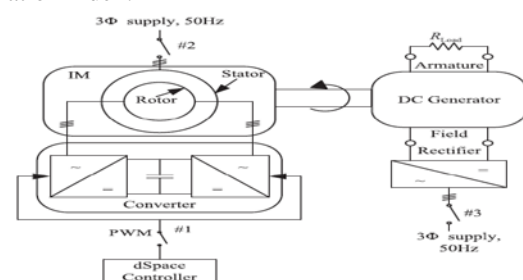


Fig. 3.1. Configuration of the system.

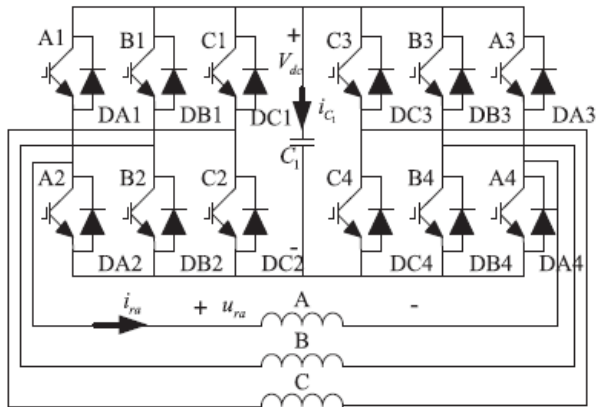


Fig. 3.2. Connection of the back-to-back converter to the rotor windings. The phase-shift angle,  $\theta_{ps}$ , between the two converters can be varied from  $-180^\circ$  to  $+180^\circ$ . A zero  $\theta_{ps}$  means that the rotor windings are short-circuited.  $\theta_{ps} = \pm 180^\circ$  means that full voltage is supplied. The dc-link voltage of the converter is not controlled but automatically balanced depending on the speed and load of the induction machine. The operating of the system can be realized in three steps. Firstly, indicated by #1 in Fig. 3.1, the switching signals are sent to the 12 power electronic valves, for instance IGBTs in this paper, A1–A4, B1–B4 and C1–C4 shown in Fig. 3.2. The fundamental frequency of the switching signals can be expressed as

$$f_2 = \frac{n_s - n_r^*}{n_s} f_1$$

where  $n_s$  and  $n_r^*$  are the synchronous and reference speed respectively while  $f_1$  is the stator frequency. Secondly, indicated by #2 in Fig. 3.1, the stator is connected to a three-phase voltage supply and the machine is started at no load. The flux generated in the stator will induce ac currents in the rotor windings. In the beginning, even though the switching signals are available, the valves cannot conduct since the dc-link voltage is zero. These currents can only flow through the anti-parallel diodes thereby charging the capacitor. The level of capacitor voltage will depend on the phase-shift angle  $\theta_{ps}$  between the two converters. If  $\theta_{ps} = 0^\circ$ , the capacitor cannot discharge through the IGBTs and its voltage will rise to a very high level. In contrast if  $\theta_{ps} = 180^\circ$ , the capacitor voltage will be low which however makes it difficult to magnetize the machine from the rotor side. In this paper  $\theta_{ps} = 60^\circ$  is used during the start of the machine. In addition, the high starting rotor current will rapidly discharge the capacitor during the acceleration of the induction machine. Thus, the capacitor voltage cannot be maintained and the converter is unable to supply a voltage of constant frequency to the rotor windings. As a result, the machine accelerates to the no load speed instead of the reference speed  $n_r^*$ . Once the machine stabilizes to its no-load steady-state speed, load torque is applied. The capacitor will be charged to a certain voltage according to the applied load and then maintain stable. Thereafter the converter can provide a three-phase voltage with slip frequency of  $f_2$  to the rotor windings. Consequently the speed of the induction machine settles to  $n_r^*$ .

4. SIMULATION RESULTS

Dynamic performance of the presented induction machine, including starting, loading and load changing, are investigated through simulation. The simulated and measured results including speed, capacitor voltage and currents in the rotor and the stator are shown in Figs. 4.2, respectively. The reference speed signals is set to 1400 r/min by controlling the fundamental frequency of IGBTs at 3.3 Hz from  $t = 0$  s. A similar starting procedure is applied both in the simulation.

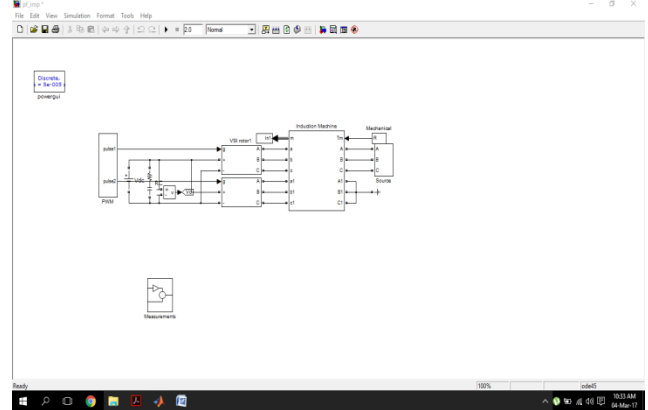


Fig:4.1 simulation diagram.

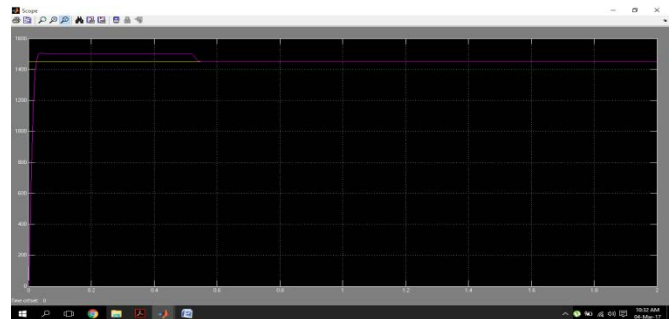


Fig:4.2(a)

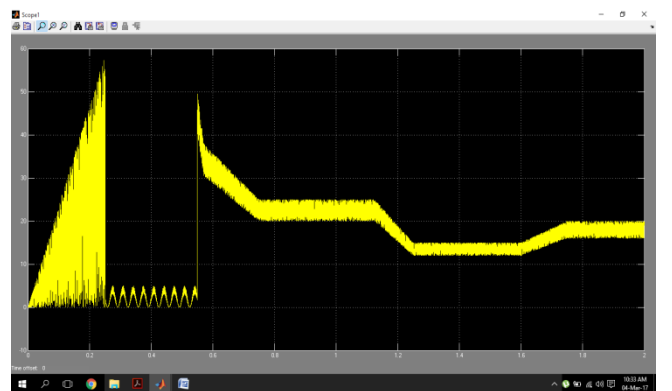


Fig:4.2(b)

The dynamic performance of the presented system is explored using MATLAB/Simulink. The Simulink model shown in Fig. 4.1 mainly consists of a wound rotor induction machine, a three-phase voltage source, a mechanical load source, two back to back connected converters fed by a PWM generation block. As can be seen in Fig. 5.1, a resistor is paralleled with the dc-link capacitor. In reality this resistor is connected in the converter for the reason of safety to protect the capacitor



from unwanted transients. It is also considered in simulation.

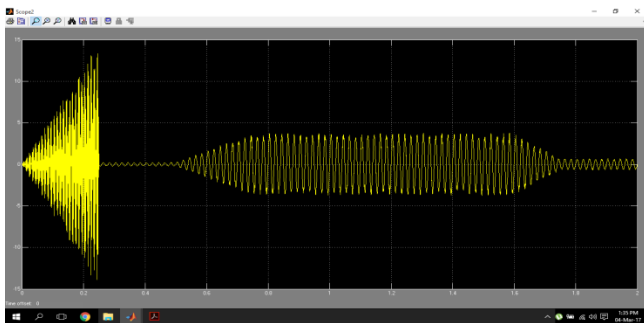


Fig:4.2(c)

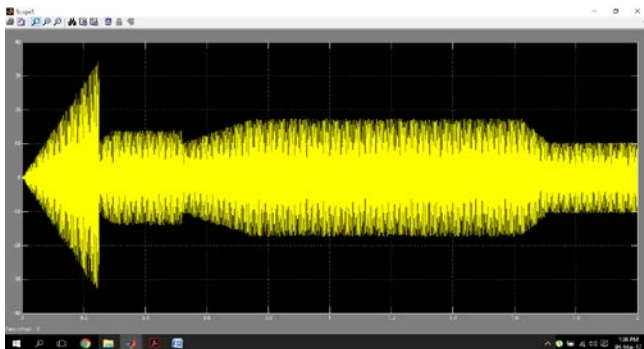


Fig:4.2(d)

Fig.4.2. Simulation results for the dynamic performance of the system: (a) Speed; (b) Capacitor voltage; (c) Rotor current of Phase A; (d) Stator current of Phase A.

In the simulation results shown in Fig. 4.2 the supply voltage is ramped from  $t = 0$  s to  $t = 4$  s at no load with  $\theta_{ps} = 60^\circ$ . The dc-link capacitor voltage is oscillating during the acceleration and the maximum value is 57V approximately. The machine accelerates to the no-load speed within around 3 s and stabilizes at the no-load speed without following the reference speed. The capacitor voltage during startup is unstable and the converter is therefore unable to provide a sufficient voltage at the frequency of 3.33 Hz to the rotor windings. The starting currents in the rotor and stator gradually rise to their maximum values, 16.5 and 34 A (peak), respectively. Note that peak values are used in following if not defined otherwise. When the speed becomes stable, the capacitor voltage declines rapidly and oscillates between 0 and 5 V due to the low no-load rotor current. The rotor current at no load steady state is 0.5A to overcome the friction. The stator current decreases to around 5A when the rotor reaches the no-load speed but gradually rises to 9A as full voltage is applied. At  $t = 10$  s, the load torque is ramped up from 0 to the rated value of 12.3N·m within 5 s. During this period the rotor current increases and charges the capacitor. At  $t = 11.4$  s the capacitor voltage is increased to its peak value of 49 V and then stabilizes to 25.7 V after  $t = 15$  s. As  $\theta_{ps} = 60^\circ$ , the converter supplies a voltage to the rotor windings. The frequency of the voltage is set to 3.33 Hz thus the speed is synchronized to 1400 r/min at around  $t = 12$  s before full load is applied. Meanwhile, the stator current rises at first but has a dip at around  $t = 11.5$  s before

it gets stable. The dip can also be seen in the measurements at around  $t = 13$  s in Fig. 4.2(d). At  $t = 22$  s,  $\theta_{ps}$  is ramped from  $60^\circ$  to  $180^\circ$  in 3 s. The capacitor voltage falls to 13.2 V and keeps oscillating with a ripple of 8 V, while the speed is kept the same. This can be seen in both the simulations and measurements. When the capacitor voltage decreases, the stator current at rated load increases from 11 to 11.8 A which are 77% and 83% of the rated current. This implies the stator power improvement of the induction machine. At  $t = 31$  s, the load torque is reduced gradually from the rated value to 0. It can be seen that even though the rotor current is decreased, Fig. 4.2(c), the capacitor voltage increases since the voltage drop on the rotor winding is reduced with the reduced current. In addition, the stator current decreases but rises again to 7.8 A after  $t = 34$  s, Fig. 4.2(d). This no-load current is lower than the current between the period 4–10 s, which is also at no load. This is because the capacitor voltage after  $t = 34$  s is around 20 V and the induction machine is then magnetized from the rotor side. Therefore the required stator current becomes less. Meanwhile it can be noted that the speed of the induction machine is kept the same during the load torque decrease. This implies that the induction machine with the rotor fed by a converter is capable to operate at constant speed and variable load.

## 5. CONCLUSION

In the presented induction machine with converter-fed rotor windings, the stator power factor can be effectively improved within a wide load range. Correspondingly, the efficiency of the induction machine is increased. The efficiency is further improved considering the losses in the power distribution network. Results for the dynamic performance including starting, loading and deloading of the induction machine are presented from simulation. It shows that the induction machine is capable of operating at constant speed and variable load by setting the fundamental frequency of the converter. The dc-link capacitor voltage is considerably low which implies a significant reduction of capacitor and converter size.

## REFERENCES

- [1] S. Das, G. Das, P. Purkait, and S. Chakravorti, "Anomalies in harmonic distortion and Concordia pattern analyses in induction motors due to capacitor bank malfunctions," in *Proc. Int. Power Syst. Conf.*, Dec. 27–29, 2009, pp. 1–6.
- [2] R. Spee and A. K. Wallace, "Comparative evaluation of power factor improvement techniques for squirrel cage induction motors," *IEEE Trans. Ind. Appl.*, vol. 28, no. 2, pp. 38–386, Mar./Apr. 1992.
- [3] N. H. Malik and A. A. Mazi, "Capacitance requirements for isolated self-excited induction generators," *IEEE Trans. Energy Convers.*, vol. EC-2, no. 1, pp. 62–69, Mar. 1987.
- [4] M. Ermis, Z. Cakir, I. Cadirci, G. Zenginobuz, and H. Tezcan, "Self excitation of induction motors compensated by permanently connected capacitors and recommendations for IEEE std 141-1993," *IEEE Trans. Ind. Appl.*, vol. 39, no. 2, pp. 313–324, Mar./Apr. 2003.
- [5] L. Ruan, W. Zhang, and P. Ye, "Unity power factor operation for three-phase induction motor," in *Proc. 3rd Int. Power Electron. Motion Control Conf.*, 2000, vol. 3, pp. 1414–1419.
- [6] E. R. Laithwaite and S. B. Kuznetsov, "Cage-rotor induction motor with unity power factor," *IEEE Proc. B Elect. Power Appl.*, vol. 129, no. 3, pp. 143–150, May 1982.

- [7] E. R. Laithwaite and S. B. Kuznetsov, "Test results obtained from a brushless unity-power-factor induction machine," *IEEE Trans. Power App. Syst.*, vol. PAS-100, no. 6, pp. 2889–2897, Jun. 1981.
- [8] "Discussion on unity-power-factor induction motors," *IEEE Proc. Elect. Power Appl.*, vol. 130, no. 1, pp. 60–68, Jan. 1983.
- [9] F. J. T. E. Ferreira and A.T. Almeida, "Novel multiflux level, three phase, squirrel-cage induction motor for efficiency and power factor maximization," *IEEE Trans. Energy Convers.*, vol. 23, no. 1, pp. 101–109, Mar. 2008.
- [10] M. V. Aware, S. G. Tarnekar, and A. G. Kothari, "Unity power factor and efficiency control of a voltage source inverter-fed variable-speed induction motor drive," *IEE Proc. Elect. Power Appl.*, vol. 147, no. 5, pp. 422–430, Sep. 2000.
- [11] M. Morimoto, K. Sumito, S. Sato, K. Oshitani, M. Ishida, and S. Okuma, "High efficiency, unity power factor VVVF drive system of an induction motor," *IEEE Trans. Power Electron.*, vol. 6, no. 3, pp. 498–503, Jul. 1991.
- [12] S. Kwak and H. A. Toliyat, "Comparison and assessment of current source- inverter-fed induction motor drive systems with unity power factor," in *Proc. IEEE 29th Annu. Ind. Electron. Soc. Conf.*, Nov. 2–6, 2003, vol. 1, pp. 232–237.